Dynamic Error Compensation Model of Articulated Arm Coordinate Measuring Machine

Jiaqi Zhu[1, a], Xugang Feng[1, b, *] and Jiayan Zhang[1, c]
[1]*School of Electrical and Information Engineering, Anhui University of Technology, Ma'anshan 243032, China*

Keywords: Neural network, Simulated annealing algorithm, Flexible arm coordinate measuring machine, Error compensation.

Abstract: The error factors of articulated arm coordinate measuring machine (AACMM) are many and the relationship between them is nonlinear, which is difficult to establish the model by traditional mathematical modeling. This paper analyses the error sources, on the basis of parameter calibration, to select the angle coding, thermal deformation and probe system as the research object and introduce coordinate values to indirectly describe the remaining errors in the model. The BP neural network is used to build up the error compensation model, connection weights of the neural network are optimized by the modified simulated annealing (MSA) algorithm, which solves the problem that the neural network is easy to fall into the local minimum and the susceptible to interference. The data samples are obtained through experiments, and the test data are utilized to exercise model built. The experimental result demonstrates that the average value of the single point repeatability error after compensation is reduced from 0.1782 mm to 0.0383 mm.

1 INTRODUCTION

The articulated arm coordinate measuring machine (AACMM) generally having 6 degrees of freedom is a non-orthogonal coordinate system measuring device that simulates the structure of the human arm. It has broad application prospects, not only can complete online measurement and evaluation on the assembly line, but also suitable for outdoor measurement and occasions where the object tested is inconvenient to move. The advantages involves of easy portability, low price, flexible measurement, large measuring range and practicality in the field. Due to its series-space open-chain structure, the measurement error has the characteristics of accumulation, transmission and amplification during the measurement process, ultimately leading to poor overall performance of the measuring machine (Zhao H N, Yu L D, Jia H K, et al, 2016; Feng X G, Xu C, Zhang J Y, et al, 2016; Fedorov V G, 2008; Romdhani F , Fran ̧ois Hennebelle, Ge M , et al, 2015; Xing H L, Bo C, Zu R Q, 2013).

At present, the AACMM mainly reduces the error by calibrating the structural parameters according to calibration algorithm or external high-precision equipment. For example, Santolaria J et al established an error model based on Fourier polynomial and estimated the parameter error of the AACMM machine by using a spherical gauge with 14 spheres (SANTOLARIA J., AGUILAR J.J. YAGUE J.A., et al, 2008). ACERO studied the feasibility of laser tracker as a reference instrument in AACMM parameter calibration (ACERO R., BRAU A., SANTOLARIA J., et al, 2015). Zheng D T established the spatial point error model and spatial error distribution of the AACMM by using the basic theory of functional network and the principle of vector machine (Zheng D T, FEI Y T, 2010).

However, there are many error factors in the AACMM, and the structural parameters are only a part of it. This paper analyzes the error sources in the measurement space and applies a method based on the improved simulated annealing algorithm to optimize the neural network to model the multiply error of the coordinate measuring machine. By comparing the results, the validity of the compensation model is verified.

2 ERROR ANALYSIS

The AACMM is composed of three joint arms and one probe combined through six rotary joints in

Zhu, J., Feng, X. and Zhang, J.
Dynamic Error Compensation Model of Articulated Arm Coordinate Measuring Machine.
DOI: 10.5220/0008856502100216
In *Proceedings of 5th International Conference on Vehicle, Mechanical and Electrical Engineering (ICVMEE 2019)*, pages 210-216
ISBN: 978-989-758-412-1

series. The structure diagram is shown in Figure 1 (Zheng D T, Fei Y T Zhang M, 2009; Cao Q S, Zhu J, Gao Z F, et al, 2010).

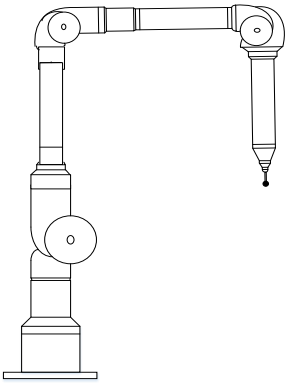

Figure 1. Schematic diagram of the AACMM.

The classical mathematical model describing the transformation relationship of adjacent members is the D-H model.

Due to the seventh coordinate system is centered on the probe , translated by the sixth coordinate system, the center of the probe is coordinated in the (x_6, y_6, z_6) coordinate system is (B_x, B_y, B_z), and the coordinate transformation matrix B is $B = [B_x \quad B_y \quad B_z \quad 1]^T$, so the spatial position coordinates of the probe relative to the base coordinate system is:

$$\begin{bmatrix} x_p \\ y_p \\ z_p \\ 1 \end{bmatrix} = \sum_{i=1}^{6} A_i B$$

$$\prod_{i=1}^{6} \begin{bmatrix} \cos\theta_i & -\sin\theta_i \cos\alpha_i & \sin\theta_i \sin\alpha_i & l_i \cos\theta_i \\ \sin\theta_i & \cos\theta_i \cos\alpha_i & -\cos\theta_i \sin\theta_i & l_i \sin\theta_i \\ 0 & \sin\alpha_i & \cos\alpha_i & d_i \\ 0 & 0 & 0 & 1 \end{bmatrix} \times \begin{bmatrix} B_x \\ B_y \\ B_z \\ 1 \end{bmatrix} \quad (1)$$

According to formula (1), the coordinate value of the probe depends on the joint angle θ, the torsion angle α , the joint length l and the joint offset d when the probe parameters are not considered (Santolaria J , Jos é-Antonio Yag üe, Roberto Jim énez, et al, 2009; Markov B N, Sharamkov A B, 2014). There are a total of 24 structural parameters. The nominal values of the structural parameters on the D-H model in this paper are shown in Table 1 But this is a static error in the AACMM, there are some additional errors usually generated in the measurement process (ZHANG T, DU L, DAI X, 2014). Thus, the error source of the measurement process of the measuring machine needs to be analysed.

Table 1. Nominal value of structural parameters.

Joint	θ_{0i} (rad)	α (rad)	l (mm)	d (mm)
1	0.111	-90..942	40.855	349.521
2	0.424	90.273	-40.562	0.723
3	-0.103	-89.821	24.588	269.051
4	-0.076	89.853	-23.877	0.812
5	0.873	-90.165	23.935	240.364
6	-0.225	90.453	-24.168	-0.162

The mainly following error sources are as follow.

(1) Thermal deformation error, caused by internal and external heat sources, resulting in errors caused by arm length, circular grating and thermal deformation of joint components. (2) The probe system error, divided into the radius cosine error of the contact probe and the error caused by the optical probe failing to accurately detect. (3) Measuring force error, mainly caused by the contact measurement force generated by the contact probe, which causes the error caused by the bending deformation of the measuring rod. (4) Angle coding error, due to the accuracy of the angle encoder itself and the error caused by assembly deviation. (5) The point error of the measurement space, because the AACMM has its optimal measurement area, the measurement is made in different measurement areas and the error caused by the difference of the position of the joint arm. (6) Data acquisition system error, due to errors caused by electromagnetic interference, data acquisition delay and its own unreliable data acquisition system in the AACMM. (7) Motion error, caused by bearing sway and unstable parts due to accuracy problems in component manufacturing and assembly in the measurement process (8) improper manual operation errors.

Through the above analysis, the AACMM is a complex system with multiple error sources. For the structural parameter error, the static parameters can be calibrated by the calibration system or the calibration algorithm. However, if all the error factors are all using the calibration method, the calculation process would be too complicated and easy to generate quadratic error. In order to better solve the influence of the remaining errors in the space and improve the measurement accuracy of the

AACMM, this paper mainly deals with the following error factors in the measurement process, which consist of thermal deformation error, angle coding error, probe system error. The temperature of the heat deformation is affected by the internal and external heat sources, and 8 thermal monitoring points are placed. 7 temperature sensors are placed on the measuring machine, and the other is the ambient temperature monitoring point. Due to the temperature characteristics, it is necessary to wait for a certain time to make the environment and the measuring machine reach the thermal balance during the experiment. The measuring head of the AACMM studied in this paper is a contact probe; there are 2 types of probe systems used in the experiment. The specific parameters are shown in Table 1. Each probe is measured the same number of times. For measurement area errors, the data samples of the measuring machine need to be measured multiple times at different locations. The influence of the measurement force error is small and it is difficult to obtain the pressure value when measuring the cone, which is combined with the other random errors indirectly described by the coordinate values in the model.

Table 2. Parameters of the probe system.

number	diameter /mm	Material	X /mm	Y /mm	Z /mm
1	4	ruby	0	0	50
2	3	ruby	0	0	40

3 MODEL

3.1 BP Neural Network

BP neural network (BP) can be regarded as a highly nonlinear mapping from input to output, and has excellent comprehensive processing capability Aiming at the problem that the AACMM has complicated error sources and the relationship between them is nonlinear, BP neural network is used to model the error of the AACMM to establish a 3-layers network with input layer, hidden layer and output layer. Based on the above analysis, there are a total of 18 neurons in the input layer, which are 6 joint angle values, the temperature of 6 joints, pedestal and the measurement space, the system type of touch probe, and the measuring coordinate value x, y, z; the number of neurons in the output layer is determined to be 3, respectively, is error values for the x-axis, y-axis, and z-axis; the number of neurons in the hidden layer is set to 2×18+3=39 according to the Kolmogorov theorem, and the transfer function uses the S-type tangent function. Therefore, the structure of the BP neural network used is 18-39-9, shown in Fig. 2. The weight value of the network is 18×39+39+39×3+3=861.

For the 3-layer neural network, the neurons in the input layer are responsible for receiving the input information and transmitting it to the neurons in the hidden layer; the hidden layer is the internal information processing layer, duty for information transformation; the output layer is responsible for outputting the information of each neuron. In the process of forward propagation, x is the neural network input, y is the neural network output, w is the weight, θ is the neural network bias, and f is the excitation function. The relationship between input and output is:

The input of hidden layer:

$$net_k = \sum_{j=1}^{n} w_{uj} x_j - \theta \tag{2}$$

The output of hidden layer:

$$y_j = f\left(net_k\right) \tag{3}$$

The input of output layer:

$$net_k = \sum_{j=1}^{n} w_{uj} x_j - \theta \tag{4}$$

The output of output layer:

$$y_k = f\left(net_k\right) \tag{5}$$

During the learning process, the neural network repeatedly adjusts the weights and thresholds of the network based on empirical results, which is accomplished by minimizing an objective function:

$$E = \frac{1}{m} \sum_{u=1}^{m} \sum_{j=1}^{l} \left(Y_{uj} - y_{uj}\right)^2 \tag{6}$$

Where: Y_{uj} is the actual output of the jth neuron, y_{uj} is the predicted output of the jth neuron, and m is the number of training samples.

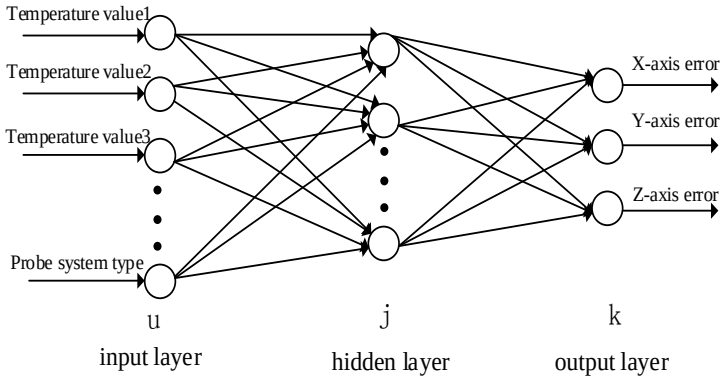

Figure 2. Model Structure of Neural Network

In the process of feedback, the formula of the gradient descent method when the weight is modified is:

$$w_{uj} = w_{uj} - \eta \nabla E\left(w_{uj}\right) \tag{7}$$

Where: η is the step size, $\nabla E\left(w_{uj}\right)$ is the partial derivative of the objective function.

3.2 Modified Simulated Annealing Algorithm

The Simulated Annealing Algorithm (SA) is derived from the annealing process of solid matter in simulated physics. It is an optimal solution for finding propositions in a large search space within a certain period of time, decomposed into three parts of solution space, objective function and initial solution. Starting from setting a higher initial temperature, a new solution is generated for the initial solution random disturbance and substituted into the energy function to determine whether the Metropolis criterion is met. If the new solution can be accepted by the system, the 'cooling' process is performed to generate the next new solution. According to the cooling coefficient, the temperature is reduced to minimize the energy function, and the global optimal solution can be obtained by receiving the temporarily deteriorated solution to jump out the local optimal "trap".

However, when SA solves nonlinear multiple parameters, the number of solutions and the solution space range is too large to make the convergence slow, and the temperature reduction in the calculation process further reduces the calculation efficiency. Thus, this paper adopts an improved simulated annealing algorithm: one is to preserve the intermediate optimal solution that can be updated in time during the algorithm search process; the second is to reduce the search range when the algorithm is close to the optimal solution to improve search efficiency and accuracy. To determine that the current state is close to the optimal solution, the following two conditions must be satisfied:

(1) The current repeatability $RP\left(\varepsilon\right)$ is less than the set value ω ; (2) The previously calculated repeatability RP is not significantly improved, meaning δRP is less than the set value ζ .

3.3 MSA-BP Model

It can be seen from the above description that the BP neural network is essentially an unconstrained nonlinear optimization process. Its learning rule is to use the descent algorithm to modify the weight through the negative gradient direction of the error function to minimize the sum of squared errors of the network, which has the disadvantages of slow convergence speed and weak anti-interference ability and easy to fall into the local minimum state. The modified annealing algorithm is used to optimize the initial weight of the BP neural network, stopping when the formula (7) is calculated to meet the set accuracy or reached the set maximum number of iterations. to obtain the optimal weight of the neural network and overcome the shortcomings of the BP neural network.

The algorithm steps are as follows:

(1)A part

Step 1: Set multiply parameters: initial temperature T_0 , initial weight $\varepsilon\left(0\right) = \varepsilon_0$, terminate test accuracy e , terminate temperature $T_{\min}$, the

threshold of checking sampling stability N , algorithm switch parameters ω and ζ , make the initial optimal solution $\varepsilon^* = \varepsilon_0$, the number of iterations $i = 0$, search range delta=delta-L;

Step 2: Let $T = T_i$, call the B algorithm with T , ε^* and $\varepsilon(i)$ as parameters, and return the state ε to the current state(mean $\varepsilon(i) = \varepsilon$) by the B algorithm, update ε^*;

Step 3: Cool down $T = T_{i+1} = \alpha T_i$, $i = i+1$;

Step 4: If $(RP\langle e \ \ or \ \ T\langle T_{\min})$, go to step 5; if $(RP\langle \omega \ \ and \ \ \delta RP\langle \zeta)$, then let delta = delta-S (delta-S < delta-L), and turn to step 2;

Step 5: Output the final optimal solution ε^*, abort the algorithm.

(2)B part

Step 1: Set the initial structural parameter $\varepsilon^{\beta}(0) = \varepsilon(i)$ when $k = 0$, and the initial optimal solution is $\varepsilon^{*\beta} = \varepsilon^*$.

Step 2: Generate a new solution by $\varepsilon^{\beta} = \varepsilon(k) + rand * delta$ and calculate $\delta RP = RP(\varepsilon^{\beta}) - RP[\varepsilon(k)]$, where rand is a random number of the interval [-1, 1], in accordance with the Cauchy distribution;

Step 3: If $\delta RP\langle 0$, then $\varepsilon(k+1) = \varepsilon^{\beta}$, $\varepsilon^* = \varepsilon^{\beta}$; if $\delta RP \geq 0$, calculate the acceptance probability $r = \exp[-RP(\varepsilon^{\beta})/T]$, if $r \rangle pp$, then $\varepsilon(k+1) = \varepsilon^{\beta}$, otherwise, $\varepsilon(k+1) = \varepsilon(k)$ pp is the random number on the interval [0, 1];

Step 4: $k = k+1$, If $k \rangle N$, go to step 5, otherwise turn to step 2.

Step 5: Return the current optimal solution ε^* and current state $\varepsilon(k+1)$ to the A algorithm.

4 EXPERIMENTAL

A standard rod where the length between cone-shape holes is 322.63 mm is placed at eight different positions in the measurement area of the AACMM. After setting several temperature ranges, AACMM starts measuring when the temperature field of the machine to be measured reaches the thermal equilibrium. The AACMM should adopt different positions while sampling the data, and the pose of length rod can by operating rotate platform in the measurement space. A total of 800 sets of data were measured, where 700 sets of it are randomly selected as the training data of the neural network. When randomly selection, the two sets of data on the rod in the same position are not separated, and the remaining 100 sets of data are used as test data to verify the predictive effect of the proposed neural network model.

In order to verify the compensation effect of the MSA-BP model, after the neural network training to reach the end condition, the 100 sets of test samples are corrected to calculate the measurement errors before and after the compensation.

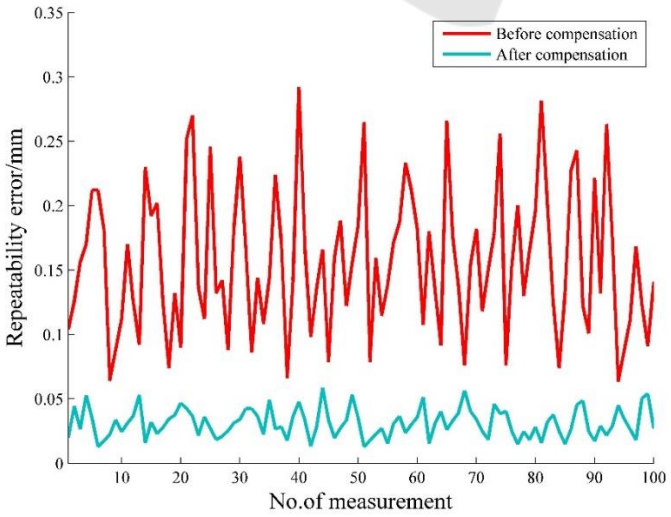

Figure 3. Repeatability error of the single cone-shape hole before and after compensation.

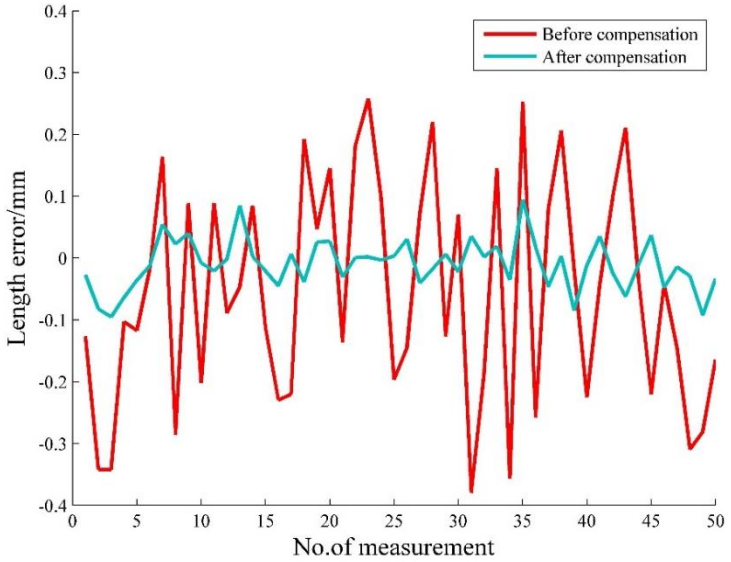

Figure 4. Length measurement errors before and after compensation.

Figure 3 shows the single point repeatability error before and after model compensation. Let the average of each set of measurement data be the true value. It can be seen from the figure that the average value of the single point repeatability error using the AACMM is 0.1782 mm, and the average value of it after the dynamic model compensation is 0.0383 mm. Figure 4 is a length measurement error diagram. The average length measurement error is reduced from -0.0681 mm m (before compensation) to -0.0085 mm (after compensation).

5 CONCLUSION

The source of measurement error of the AACMM is analyzed, due to the lack of the unified error calculation formula, a dynamic error compensation method based on MSA-BP for AACMM is proposed. The BP neural network is used as the error compensation model of the AACMM, the weight of which is optimized by adopting the modified simulated annealing algorithm, which improves the convergence speed and operation efficiency. The simulation results show that the average value of the repeatability error based on the parameter calibration is 0.1782mm. After compensation of the MSA-BP model, the average value of the repeated error is 0.0383mm. The dynamic error compensation model presented in this paper can effectively improve the accuracy of the AACMM and has good engineering application value.

ACKNOWLEDGEMENTS

This paper was supported by Anhui Natural the Science Foundation (No.1908085ME134), by Anhui Key Research and Development Plan Project (No.1804a09020094) and by the key research project of Natural Science in Anhui University (No.KJ2018A0054, KJ2018A0060).

REFERENCES

ACERO R., BRAU A., SANTOLARIA J., et al. Verification of an AACMM using a laser tracker as reference equipment and an indexed metrology platform[J]. Measurement, 2015, 69: 52- 63.

Cao Q S, Zhu J, Gao Z F, et al. Design of Integrated Error Compensating System for the Portable Flexible CMMs[M]// Computer and Computing Technologies in Agriculture IV. Springer Berlin Heidelberg, 2010:410-419.

Fedorov V G. Six-axis coordinate measuring machines [J]. Measurement Techniques, 2008, 51(7):724-725

Feng X G, Xu C, Zhang J Y, et al. The establishment and testing of a model called virtual AACMM [J]. Journal of Chongqing University, 2016, 39(06):135-140.

Markov B N, Sharamkov A B. The Use of the Results of Calibration of Faro Arm Coordinate-Measuring Machines for Use in Comparative Estimation of Their Precision Capabilities [J]. Measurement Techniques, 2014, 57(8):870-874.

Romdhani F, François Hennebelle, Ge M, et al. Methodology for the assessment of measuring uncertainties of AACMMs [J]. Measurement Science & Technology, 2015, 25(25):125008.

SANTOLARIA J., AGUILAR J.J.,YAGUE J.A., et al. Kinematic parameter estimation technique for calibration and repeatability improvement of AACMM[J]. Precision Engineering, 2008, 32(4): 251-168.

Santolaria J, José-Antonio Yagüe, Roberto Jiménez, et al. Calibration-based thermal error model for AACMMs [J]. Precision Engineering, 2009, 33(4):476-485.

Xing H L, Bo C, Zu R Q. The calibration and error compensation techniques for an Articulated Arm CMM with two parallel rotational axes [J]. Measurement, 2013, 46(1):603-609.

ZHANG T, DU L, DAI X. Test of Robot Distance Error and Compensation of Kinematic Full Parameters [J]. Advances in Mechanical Engineering, 2014, 2014 (22):1-9.

Zhao H N, Yu L D, Jia H K, et al. A New Kinematic Model of Portable Articulated Coordinate Measuring Machine [J]. Applied Sciences, 2016, 6(7):181.

Zheng D T, FEI Y T. Research on Spatial Error Model of Flexible Coordinate Measuring Machine [J]. Journal of Mechanical Engineering, 2010, 46(10):19-24. (In Chinese)

Zheng D T, Fei Y T Zhang M. Research on functional networks of flexible coordinate measuring machine modelling [J]. Journal of Electronic Measurement and Instrument, 2009, 23(04): 33-37. (In Chinese)